



Acetyl analogs of combretastatin A-4: Synthesis and biological studies

Balaji Babu^a, Megan Lee^a, Lauren Lee^a, Raymond Strobel^a, Olivia Brockway^a, Alexis Nickols^a, Robert Sjöholm^a, Samuel Tzou^a, Sameer Chavda^a, Dereje Desta^b, Gregory Fraley^b, Adam Siegfried^c, William Pennington^c, Rachel M. Hartley^d, Cara Westbrook^d, Susan L. Mooberry^{d,e}, Konstantinos Kiakos^f, John A. Hartley^f, Moses Lee^{a,*}

^a Department of Chemistry and the Division of Natural and Applied Sciences, Hope College 49423, USA

^b Department of Biology, Hope College 49423, USA

^c Department of Chemistry, Clemson University, SC 29634, USA

^d Department of Pharmacology, University of Texas Health Science Center at San Antonio, San Antonio, TX 78229, USA

^e Department of Medicine, University of Texas Health Science Center at San Antonio, San Antonio, TX 78229, USA

^f UCL Cancer Research Institute, University College London, Paul O' Gorman Building, 72 Huntley Street, London WC1F 6BT, UK

ARTICLE INFO

Article history:

Received 21 December 2010

Revised 9 February 2011

Accepted 11 February 2011

Available online 17 February 2011

Keywords:

Combretastatin A-4

Trimethoxyphenylacetone

Tubulin

Microtubule

Cytotoxicity

Cancer

ABSTRACT

The combretastatins have received significant attention because of their simple chemical structures, excellent antitumor efficacy and novel antivascular mechanisms of action. Herein, we report the synthesis of 20 novel acetyl analogs of CA-4 (**1**), synthesized from 3,4,5-trimethoxyphenylacetone that comprises the A ring of CA-4 with different aromatic aldehydes as the B ring. Molecular modeling studies indicate that these new compounds possess a 'twisted' conformation similar to CA-4. The new analogs effectively inhibit the growth of human and murine cancer cells. The most potent compounds **6k**, **6s** and **6t**, have IC₅₀ values in the sub- μ M range. Analog **6t** has an IC₅₀ of 182 nM in MDA-MB-435 cells and has advantages over earlier analogs due to its enhanced water solubility (456 μ M). This compound initiates microtubule depolymerization with an EC₅₀ value of 1.8 μ M in A-10 cells. In a murine L1210 syngeneic tumor model **6t** had antitumor activity and no apparent toxicity.

© 2011 Elsevier Ltd. All rights reserved.

1. Introduction

The ongoing efforts of US National Cancer Institute to identify anticancer agents of natural origin led to the identification of combretastatins, which were initially isolated from the African willow tree *Combretum caffrum* (Combretaceae). The most potent of these initial combretastatins was combretastatin A-4 (CA-4 or **1**, Fig. 1).¹ CA-4 is an antimitotic agent that binds to the colchicine site on tubulin causing inhibition of tubulin polymerization and in cells microtubule depolymerization and mitotic accumulation.² CA-4 (**1**) exhibits potent cytotoxicity against a broad spectrum of human cancer lines, including those that are multidrug resistance (MDR) positive.³ This compound also elicits irreversible vascular shut-down in solid tumors, leaving normal vasculature intact, thereby acting as a vascular disrupting agent.⁴ Major limitations of **1** are its poor aqueous solubility and bioavailability, which significantly impairs optimal in vivo antitumor activity.⁵ The relative simplicity of the 1,2-diarylethene scaffold of the CA-4 series, along with their biological properties, resulted in extensive structure–activity

relationship (SAR) studies of CA-4 analogs. Consequently, it was found that a 3,4,5-trimethoxyphenyl as the A ring substituents and a *cis* disposition of the double bond between two aryl groups (A and B) is optimal for biological activities. Many analogs of **1** have been developed over time that can retain the biological actions of the parent molecule but that have improved water solubility and better pharmacokinetic properties. These analogs include a water-soluble phosphate prodrug derivative of CA-4, CA-4P (**2**), as well as AVE 8062 (**3**) and the amino derivative AC-7739 (**4**) (Fig. 1). CA-4P (Zybrestat), CA-1 diphosphate (Oxi4503), AVE 8062 and NPI-2358 are currently being evaluated in clinical trials. Another class of compound where the two aryl rings are bridged through three atoms is represented by A-105972 (**5a**, Fig. 1), an oxadiazoline analog, which exhibits potency towards multidrug resistant cancer cells.⁶ Another cytotoxic oxadiazoline compound **5b** (Fig. 1) was developed in the authors' laboratory, and it was found to cause microtubule depolymerization.^{7e}

Our work has recently focused on the synthesis of novel CA-4 analogs that retain the cytotoxic and microtubule disrupting activities of the parent molecule (**1a**). However, we have not yet identified an analog that preserves the cytotoxic potency of CA-4.⁸ We recently reported the synthesis and cytotoxicity of α,β -unsaturated

* Corresponding author. Tel.: +1 616 395 7190.

E-mail address: lee@hope.edu (M. Lee).

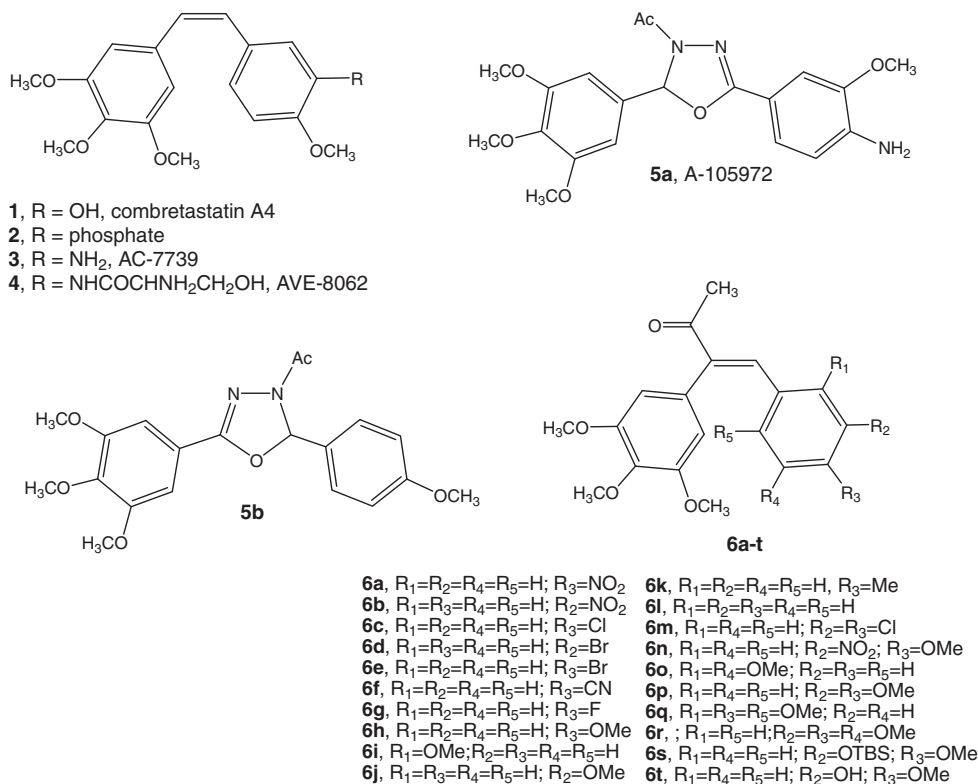


Figure 1. Structures of combretastatin A-4 (CA-4, **1**), CA-4 phosphate derivative, **2**, amino acid analog of CA-4, **3** (AVE-8062), amino analog of CA-4, **4** (AC-7739), oxadiazoline analogs A-105972 (**5a**), **5b** and novel acetyl combretastatin analogs reported herein **6a–6t**.

ketone analogs of CA-4 from simple phenylacetone, which showed modest activity against L1210 and B16 cancer cells.^{7d} However, those compounds did not contain the 3,4,5-trimethoxyphenyl A ring normally found in combretastatin analogs. The goal of this study was to design novel structures that contained a 3,4,5-trimethoxyphenyl group. Accordingly, 20 novel acetyl-CA-4 analogs **6a–t** (Fig. 1) containing the 3,4,5-trimethoxyphenyl group A ring and a variety of aromatic aldehydes as the B ring were synthesized. Compounds **6a–t** were tested for their cytotoxicity against L1210 and B16 cell lines and for effects on cellular microtubules. The *in vivo* antitumor activities were evaluated for the most potent compounds **6k** and **6t**.

2. Results and discussion

2.1. Chemistry

Compounds **6a–t** were prepared through the Claisen–Schmidt condensation of 3,4,5-trimethoxyphenylacetone with the appropriate aldehydes using piperidine and benzoic acid as catalysts (Scheme 1). The starting material 3,4,5-trimethoxyphenyl acetone was prepared as described previously.⁹ In general, the phenolic group was protected using TBDMSCl (*tert*-butyldimethylsilyl chloride) during the reaction and was regenerated by using 1 M TBAF in THF after the reaction. The yields range from 15% to 96% after purification by silica gel column chromatography.

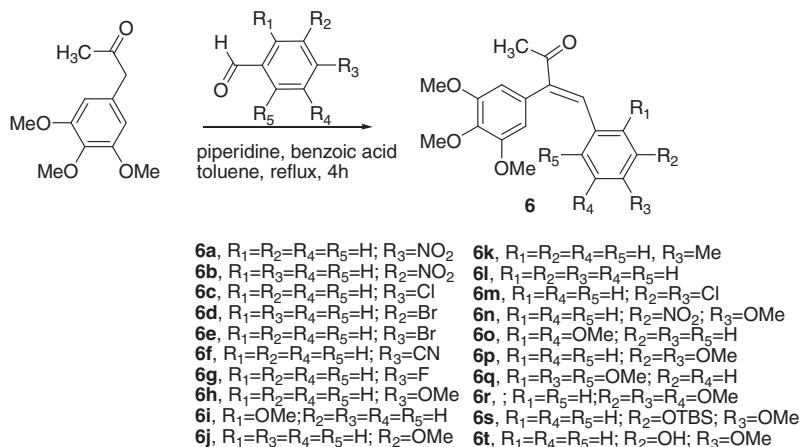
2.2. Conformation

Confirmation of the *cis* configuration about the double bond between the A and B rings was achieved with a single X-ray crystallographic analysis of the nitro compound **6a** (Fig. 2). The chemical shift of the β -vinylic proton in the ¹H NMR spectra at 7.58 ppm

correlates with literature precedence,^{7d} thereby, providing support for the *cis* geometry. The conformation of compounds **6a** and **6t** were also examined by molecular modeling studies using the suite of programs in MacSpartan, version '04. Upon optimization of the structure using molecular mechanics (MMFF) and molecular dynamics (equilibrium conformer search option and molecular mechanics), the structure was energy optimized using Hartree–Fock (3-21G) calculations, followed by density function theory (B3LYP and 6-31G⁺) calculations. The conformation of CA-4 (**1**) has been previously reported using the same protocol,¹⁰ and was used for comparison purposes in this study. The determined conformations of the compounds **6a**, **6t** and **1**, depicted in Figure 3, are remarkably similar to the X-ray structure of **6a**. It is evident from these results that due to the steric hindrance in the *cis*-stilbene framework the molecule adopts a slightly 'twisted' conformation. According to the X-ray crystal structure and the molecular models of compound **6a** and **6t**, the 4-nitrophenyl-3-buten-2-one sub-structure is held relatively planar ($\sim 7^\circ$) and the trimethoxyphenyl group rotates by $\sim 60^\circ$ about the alkene to minimize steric hindrance between the two aromatic units. The conformation is similar to that observed in the X-ray structure¹¹ and molecular model of CA-4 suggesting these compounds are capable of exhibiting a similar tubulin-targeting mechanism of action.

2.3. Solubility assay

To test our assumption that adding an acetyl group increases water solubility, a solubility assay was conducted. The aqueous solubility of **6h**, **6k** and **6t** were measured using a modified version of the Multiscreen Solubility filter plate protocol developed by Millipore.^{7e} The maximum aqueous solubility for this assay is 500 μ M. Two independent experiments were conducted and the data indicate that the aqueous solubility of **6h** is 319 μ M and **6k** is



Scheme 1. Synthesis of acetyl-combretastatin analogs **6a–t**.

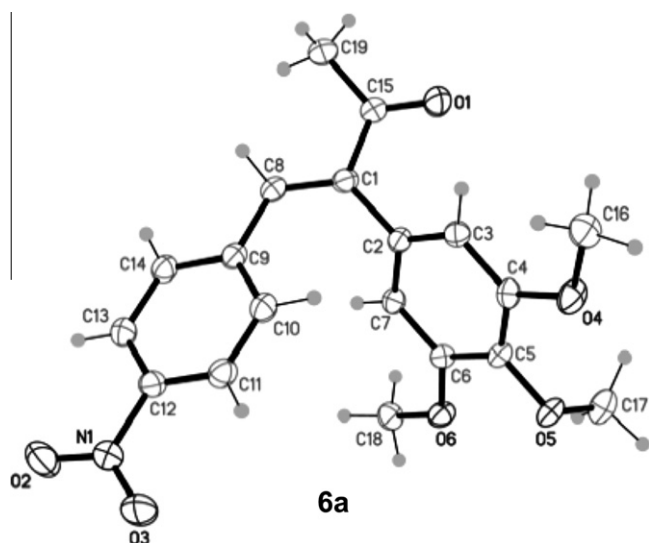


Figure 2. X-ray structure of compound **6a**. Complete X-ray structural data for **6a** were deposited with the Cambridge Crystallographic Data Centre (CCDC deposition number: 811797).

443 μM . The analog **6t** has an aqueous solubility of 456 μM , indicating that the addition of an acetyl group on the ethenyl moiety increases the aqueous solubility of the compound when compared to CA-4 itself and acetyl oxadiazoline **5b**.^{7e}

2.4. Cytotoxicity

The compounds were evaluated for cytotoxic activity against murine B16 melanoma and L1210 leukemia cells. The results,

shown in **Table 1**, show several interesting trends based upon the substitution pattern of the aromatic ring B. The compound **6l** (derived from benzaldehyde), yielded IC₅₀ values of 25 and 5.4 μM against B16 and L1210 cells, respectively. For the B ring monosubstituted compounds (**Table 1**), a nitro group in the *meta*-position (**6b**) yielded good potency against L1210 and B16 cells (IC₅₀ 3.8 and 3.3 μM , respectively). Moving this nitro group to the *para*-position (**6a**) lowered the potency 4 to 5-fold against both cell lines in comparison to **6b**, suggesting that the electronic influence (due to inductive effects) of the *meta*-nitro group enhances the interaction of **6b** with its cellular targets. In contrast, the compounds with halogens in the *meta*- and *para*-position (**6c–6e** and **6g**) showed modest to poor activity (IC₅₀ values in the range of 7.4–65 μM), with **6c** and **6e** (containing *para*-chloro and *para*-bromo substituents, respectively) exhibiting the highest potency against one or both cell lines. Interestingly, incorporation of the slightly less polar and larger bromo substituent at the *meta*-position in **6d** (in comparison to **6c**) resulted in additional loss of cytotoxic potency in both cell lines (IC₅₀ values of 39 and 35 μM in B16 and L1210 cells, respectively). Similar trends (based upon substitution pattern) seem apparent for compounds **6h–6k** (**Table 1**). Electron-donating methoxy and methyl substituents in the *para*-position (**6h** and **6k**) increased potency against cell lines and gave IC₅₀ values for L1210 cells in the sub- μM range; 0.38 and 0.36 μM , respectively. Only modest levels of cytotoxicity were observed for **6i** and **6j**. This suggests that substituent size is a factor contributing to the potency of these compounds, as could substituent polarizability in the *para*-position. Based upon the information obtained from the study of the monosubstituted compounds, we were curious to ascertain whether some of the trends observed for monosubstituted compounds could be enhanced via incorporation of two substituents into the aromatic ring. In comparison to **6b**, **6c** and **6h**, similar

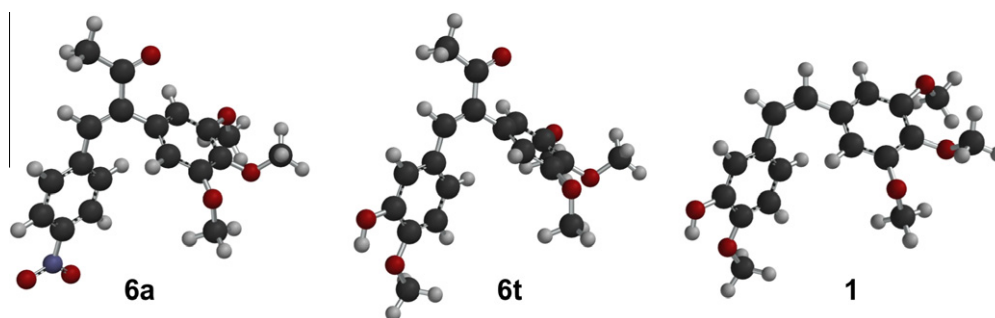
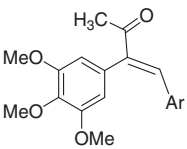
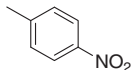
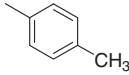
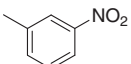
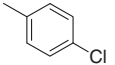
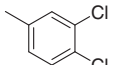
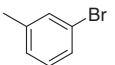
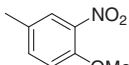
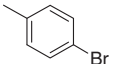
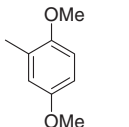
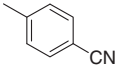
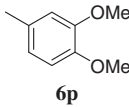
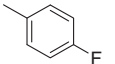
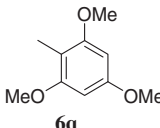
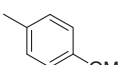
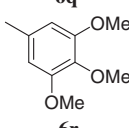
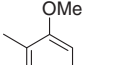
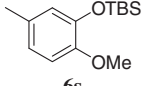
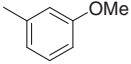
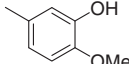


Figure 3. Molecular models of compounds **6a**, **6t**, and CA-4, **1**.

Table 1
Cytotoxicity of the compounds **6a–6t** on L1210 and B16 cancer cell lines

Compound	IC ₅₀ (μM)		IC ₅₀ (μM)	
	B16	L1210	B16	L1210
				
Ar =				
 6a	18 ± 7.8	18 ± 9.2	 6k	2.9 0.36
 6b	3.8 ± 0.3	3.3 ± 0.2	 6l	25 ± 4.2 5.4 ± 0.2
 6c	7.4 ± 2.5	5.0 ± 0.1	 6m	6.4 ± 1.2 4.0
 6d	39 ± 1.4	35 ± 6.4	 6n	3.8 ± 0.2 3.1
 6e	19 ± 9.2	4.0 ± 1.5	 6o	4.0 ± 0.1 3.7 ± 0.01
 6f	29 ± 12	8.0 ± 4	 6p	42 ± 4.9 37 ± 11.3
 6g	65 ± 7.1	43 ± 4.2	 6q	>100 3.7 ± 0.9
 6h	7.3 ± 1.7	0.38	 6r	23 ± 2.8 7.2 ± 2
 6i	41 ± 13.4	40	 6s	5.1 ± 2.9 0.18
 6j	31 ± 0.7	39 ± 0.7	 6t	3.5 ± 1.4 0.45 ± 0.1

IC₅₀ values are expressed in μM.

cytotoxic potency for the disubstituted counterparts **6m** (containing chlorine atoms in both the *meta*- and *para*-positions) and **6n** (*meta*-nitro and *para*-methoxy) were observed, confirming the trends seen with the mono substituted compounds. The molecules **6q** and **6r** which contain trisubstituted methoxy groups in the 2,4,6 and 3,4,5 positions (Table 1) showed no significant activity against either cell line, suggesting that the steric congestion resulting from multiple methoxy groups prevents optimal orientation within the binding site as compared to the analogs **6h** and **6k**. The synthesized exact acetyl analogs of CA-4 **1** (**6s** and **6t**) showed significant

activity (IC₅₀ in 0.18–3.5 μM range, Table 1). Finally, the enhanced potency of some of these molecules towards leukemia cells (L1210) over solid tumor cells (B16) is, in general, consistent with studies on other combretastatin analogs from our laboratory.^{7,12}

2.5. NCI data

Compound **6t** was evaluated at the National Cancer Institute against a panel of 60 human cancer cell lines.¹³ Inhibition of cell proliferation after 48 h continuous exposure was determined using

the sulforhodamine B assay. The GI₅₀ values (the concentration for cell growth inhibition by 50%) for compound **6t** against the panel are shown in Figure 4. Bars extending to the right indicate cell lines that are more sensitive than average to **6t**, whereas bars extending to the left indicate less sensitive cell lines. Interesting observations were made on these results. First, **6t** exhibited selectivity against certain leukemia, ovarian, colon, melanoma and renal cancer cell lines. It showed extremely high activity against the MDA-MB 435 melanoma cell line. Second, the TGI (the concentration for total cell growth inhibition) indicates that it is highly active against some non-small lung cancer, colon cancer, CNS cancer, ovarian cancer, renal cancer, prostate cancer, breast cancer and the most potent against MDA-MB-435. In a separate study using a previously published procedure,^{7e} the IC₅₀ values for compounds **6h**, **6k**, and **6t** against MDA-MB-435 were found to be 0.35, 0.095, and 0.182 μM, respectively, indicating that acetyl-CA4 analogs are viable cytotoxic agents worthy of further studies.

2.6. Microtubule depolymerization activity

To evaluate the cellular mechanism of action, the effects of **6b**, **6c**, **6h**, **6k**, **6n**, and **6t** on interphase cellular microtubules were

evaluated in A-10 cells, a non-transformed cell line that arrests in interphase in response to microtubule targeting agents.^{7e,14} Only **6h**, **6k** and **6t** showed significant microtubule depolymerization activity at concentrations below 30 μM (see Fig. 5). A range of concentrations was evaluated for compounds **6h**, **6k**, **6t** and the EC₅₀ values, the concentration required to cause 50% loss of cellular microtubules, as visualized by microscopy was calculated and the values were found to be 18.6, 5.6 and 1.8 μM, respectively. The data were further analyzed by calculating ratios of these EC₅₀ values and IC₅₀ against MDA-MB-435 cells. In this analysis, the linkage of microtubule depolymerizing and cytotoxic effects can be compared among large groups of compounds. Tight linkage is seen with CA-4, which gives a ratio of 2–3 in these assays.^{7e} The ratios were found to be 53, 59, and 10 for **6h**, **6k** and **6t**, respectively. This ratio suggests that the acetyl-analog **6t** of this series has a mechanism of action closest to the CA-4. In contrast, the significantly higher ratios of compounds **6h** and **6k** suggest microtubule disruption is not the only mechanism of cytotoxicity. This is not surprising since analogs of combretastatins have been found to bind to other biological targets, such as the kinesin spindle protein (KSP)¹⁵ and DNA.¹⁶

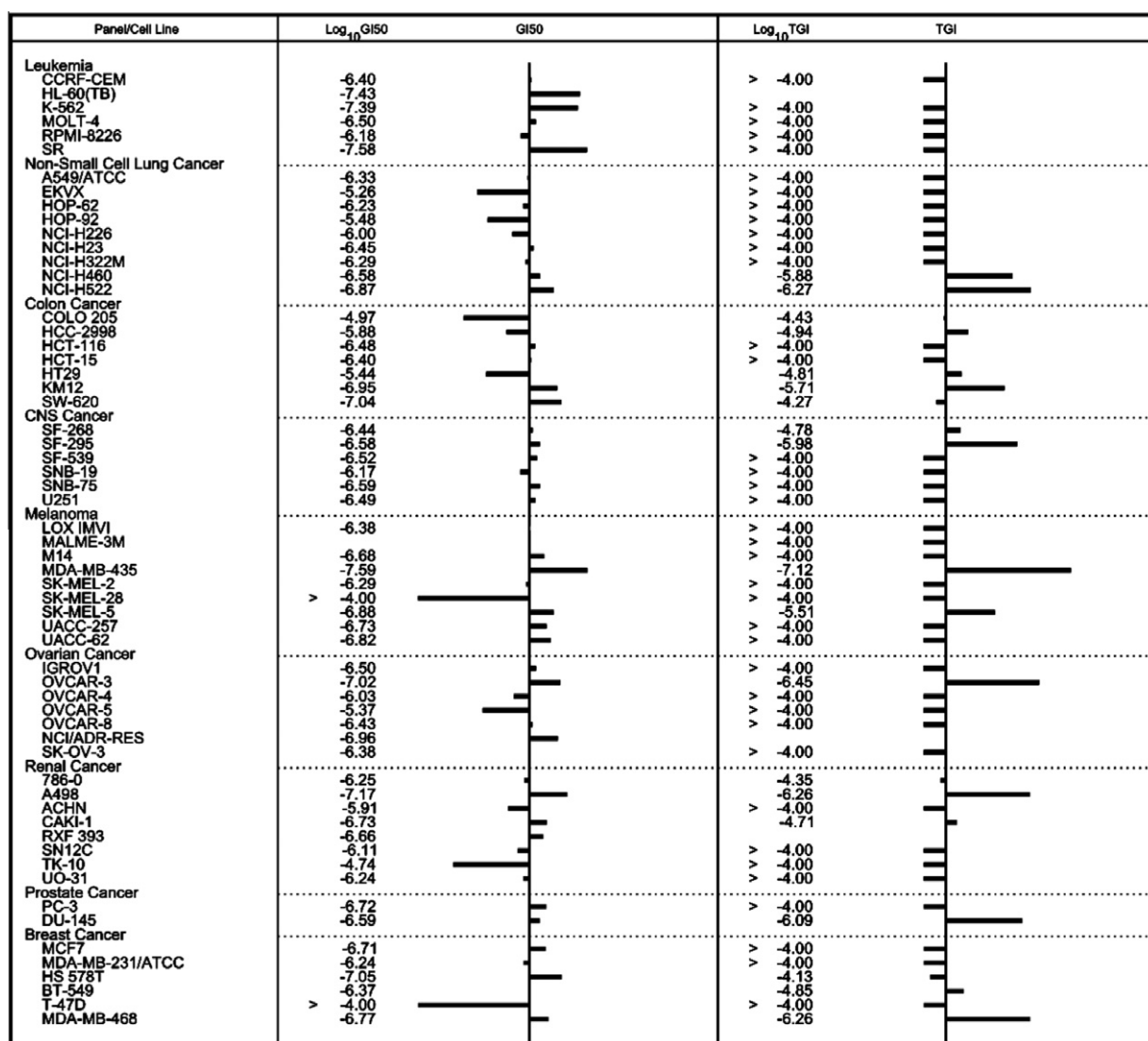


Figure 4. NCI 60-cell line screen data (GI₅₀ and TGI values) for **6t** against a panel of human cancer cell lines. GI₅₀ is the concentration needed to inhibit the growth of cancer cells by 50%. TGI is total growth inhibition.

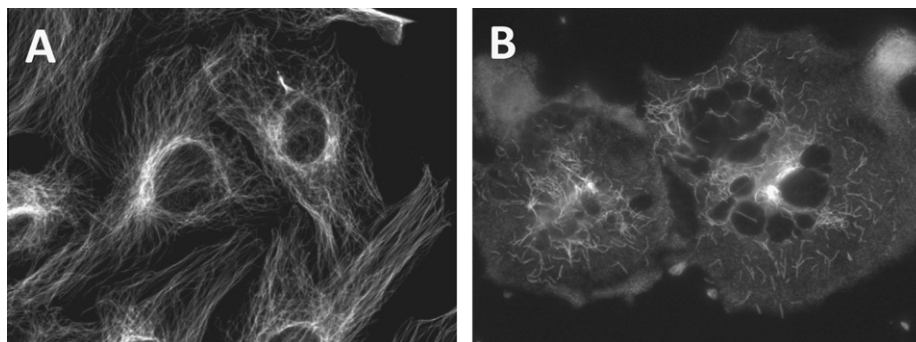


Figure 5. Effects of **6t** on cellular microtubules. A-10 cells were treated for 18 h with vehicle (A) or 4.5 μM **6t** (B) and cellular microtubule structures visualized with indirect immunofluorescence techniques. Panel A shows the normal interphase microtubules are visible. Panel B shows the **6t**-induced loss of interphase microtubules.

2.7. In vivo studies of **6k** and **6t** against DBA2 mice

Compounds **6k** and **6t** were evaluated for toxicity against female DBA2 mice using a dose of 75 mg/kg. Five mice were used on each test group. The compounds were administered via intraperitoneal (ip) injections on days 1, 5, 9, 13, and 17. The body weights of the mice over the course of the experiment are shown in Figure 6 and indicate that similar to the control vehicle-treated mice neither compound caused significant body weight loss, which is indicative of negligible systemic toxicity over 19 days. At the end of the experiment (day 23), all the animals were euthanized and the blood and vital organs (kidney, liver, and spleen) were examined. Compared to the vehicle-treated controls, the vital organs appear the same in terms of color, weight, and size, indicating negligible toxicity to the animals. Blood chemistry including hematocrit, white blood count, granulocyte count and platelet count was evaluated. Again, comparing to the vehicle control, no significant difference was observed for the drug-treated animals. Collectively, these results provided preliminary evidence that compounds **6k** and **6t**, formulated and dosed as described above do not cause systemic toxicity of a 23-day period.

A preliminary in vivo antitumor study on compound **6t** was initiated using four female DBA2 mice per test group. The mice were inoculated on day 0 with 2×10^5 L1210 cells on the right flank. The

vehicle used to formulate the samples was identical to that used in the toxicity experiment, as was the ip route and volume of injection. The animals were treated at a dose of 50 mg/kg of compound **6t** once a day, starting on day 1 and continued on days 3, 5, 7, 9, 11, 13, 15, and 17. This dose was chosen with the purpose of keeping the total mass of the compound close to that used in the toxicity study. Another group of four mice were administered with only the vehicle and that provided a negative control group for the study. On day 23, the flank tumors on animals treated with **6t** were on average reduced by 35% compared than those on the control animals, indicating that compound **6t** has some in vivo antitumor activity.

3. Conclusion

Twenty novel acetyl-combretastatin analogs were designed and synthesized with good yields. Incorporation of an acetyl functionality enhanced water solubility as compared to CA-4 and ease of synthesis. Acetyl-containing compounds possess good cytotoxic potency and **6t** appears to retain the microtubule disrupting mechanism of action of CA-4. Compound **6t** at a dose of 75 mg/kg given five times, over 19 days was found to be non-toxic in mice, and according to a preliminary study, it produced some antitumor effect on the growth of L1210 grown on the right flank in mice. Fur-

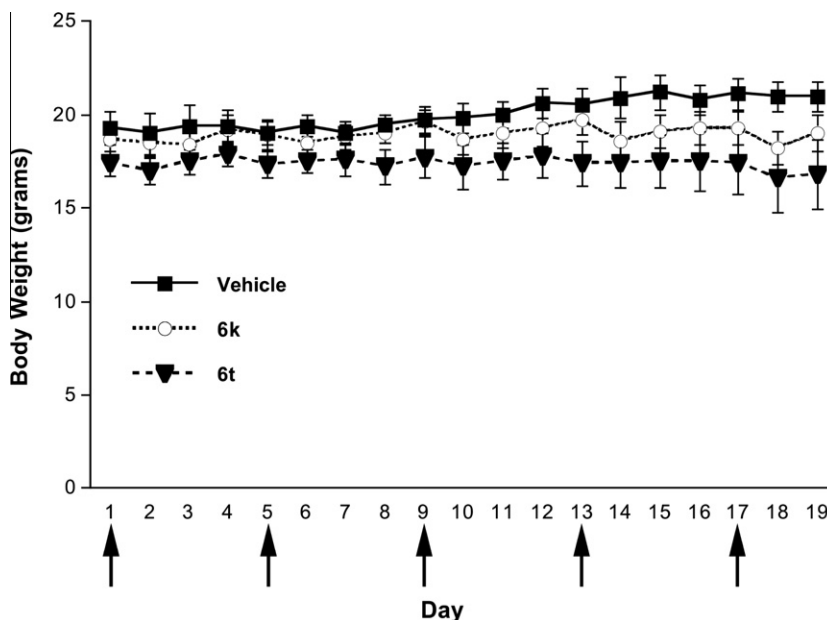


Figure 6. Toxicity studies. Change in body weight of mice treated with vehicle control (solid square) and 75 mg/kg dose of **6k** (open circle) or **6t** (solid triangle) given five times over 19 days as indicated by the arrows.

ther investigations are underway to continue to improve **6t** in relation to increasing potency and aqueous solubility, and maintaining the anti-tubulin mechanism of action.

4. Experimental

4.1. Synthesis

4.1.1. General

Solvents and organic reagents were purchased from Aldrich or Fischer, and were used without further purification. Melting points (mp) were performed using a Mel-temp instrument and the results were not corrected. Infrared (IR) spectra were recorded using a Midac M1700 FT-IR instrument as films on KBr discs unless stated otherwise. Proton NMR spectra were recorded on a Varian INOVA 400 MHz Fourier transform spectrometer using an internal deuterium lock. Chemical shifts are quoted in parts per million downfield from tetramethylsilane. High-resolution mass spectra (HRMS) and low-resolution mass spectra (LRMS) were provided by the Mass Spectrometry Laboratory, University of South Carolina, Columbia, SC. The single crystal X-ray diffraction studies on compound **6a** were performed at Clemson University, Clemson, SC, in the laboratory of Professor William Pennington. Reactions were monitored using thin-layer chromatography (TLC) using commercially available pre-coated plates (Merck Kieselgel 60 F254 silica). Visualization was achieved with UV light at 254 nm, I₂ vapor staining and ninhydrin spray.

4.1.2. General procedure for the synthesis of **6a–t**

To a solution of 3,4,5-trimethoxyphenyl acetone (1 equiv) and aromatic aldehyde (1 equiv) in toluene was added benzoic acid (1 equiv) followed by piperidine (0.02 equiv). The solution was refluxed for 4 h. TLC showed disappearance of starting materials. The solvent was removed under vacuum using rotary evaporator. The residue was purified by column chromatography using hexane (100:0) and ethyl acetate (0:100).

4.1.3. Compound **6a**

Color: orange yellow solid (62%); $R_f = 0.2$ (50% ethyl acetate/hexane); mp 145–147 °C; IR (KBr disc)/cm⁻¹ 2940, 2838, 1709, 1592, 1552, 1518, 1508.56, 1456, 1415, 1378, 1344, 1238, 1126, 1068, 1005, 861, 834, 722, 669; ¹H NMR (400 MHz, CDCl₃): δ 8.07 (d, $J = 8.0$ Hz, 2H), 7.58 (s, 1H), 7.24 (d, 2H), 6.35 (s, 2H), 3.92 (s, 3H), 3.77 (s, 6H), 2.37 (s, 3H); LRMS: EI+ 357 (100% M⁺).

Crystallographic data for **6a**: C₁₉H₁₉NO₆, $M = 357.35$, monoclinic, C2/c (#15), $a = 30.6394(12)$, $b = 7.2842(4)$, $c = 18.4845(7)$ Å, $\beta = 124.045(9)^\circ$, $V = 3418.3(3)$ Å³, $Z = 8$, $D_c = 1.39$ g cm⁻³, $\mu(\text{Mo K}\alpha) = 0.104$ mm⁻¹, light yellow parallelepiped crystal, $0.22 \times 0.27 \times 0.31$ mm, $F(000) = 1504$. Data collection at 163(2) K on a Rigaku Mercury/AFC8 diffractometer yielded 15555 reflections ($2.21 < \theta < 26.35^\circ$) of which 3480 were unique ($R_{int} = 0.025$) and 3021 were observed ($I > 2\sigma(I)$). Structure solution and refinement were performed with SHELXTL (version 6.10). Final residuals: $R_1 = 0.043$, $wR_2 = 0.107$, $R_1(\text{all data}) = 0.050$, $wR_2(\text{all data}) = 0.114$, $S = 1.06$. The crystals were grown by slow evaporation of an ethyl acetate/hexane solution (50:50). The molecules are linked by several weak C–H...O interactions with a C...O distance range of 3.179(2)–3.6393(18) Å (average of 3.42(14) Å). CCDC deposition number: 811797. This data can be obtained free of charge from The Cambridge Crystallographic Data Centre via www.ccdc.cam.ac.uk/data_request/cif.

4.1.4. Compound **6b**

Color: yellow oil (15%); $R_f = 0.32$ (50% ethyl acetate/hexane); IR (KBr disc)/cm⁻¹ 2996, 2961, 2938, 2832, 1708, 1687, 1671, 1581,

1529, 1462, 1455, 1412, 1350, 1307, 1287, 1237, 1198, 1182, 1125, 1006, 920, 876, 809, 774, 735, 675; ¹H NMR (400 MHz, CDCl₃): δ 8.05–8.09 (m, 1H), 7.97 (s, 1H), 7.61 (s, 1H), 7.39 (m, 2H), 6.38 (s, 2H), 3.86 (s, 3H), 3.79 (s, 6H), 2.39 (s, 3H); LRMS: EI+ 357 (100% M⁺); HRMS: obs = 357.1211; calcd = 357.1212.

4.1.5. Compound **6c**

Color: off white solid (43%); $R_f = 0.62$ (50% ethyl acetate/hexane); mp 99–101 °C; IR (KBr disc)/cm⁻¹ 2996, 2959, 2936, 2829, 1721, 1667, 1580, 1558, 1538, 1503, 1490, 1462, 1452, 1410, 1353, 1316, 1300, 1275, 1235, 1195, 1181, 1126, 1090, 1011, 974, 876, 818, 772, 745, 679; ¹H NMR (400 MHz, CDCl₃): δ 7.54 (s, 1H), 7.16 (d, $J = 8.0$ Hz, 2H), 7.00 (d, $J = 8.0$ Hz, 2H), 6.35 (s, 2H), 3.90 (s, 3H), 3.77 (s, 6H), 2.34 (s, 3H); LRMS: EI+ 347 (100% M⁺).

4.1.6. Compound **6d**

Color: orange oil (98%); $R_f = 0.32$ (50% ethyl acetate/hexane); IR (KBr disc)/cm⁻¹ 3063, 2997, 2939, 2837, 1960, 1710, 1669, 1590, 1505, 1462, 1432, 1354, 1341, 1312, 1273, 1183, 1154, 1127, 1075, 1040, 1007, 923, 881, 834, 781, 752, 688, 669; ¹H NMR (400 MHz, CDCl₃): δ 7.50 (s, 1H), 7.35 (d, $J = 8.0$ Hz, 1H), 7.24 (s, 1H), 7.05 (t, $J = 8.0$ Hz, 1H); 6.92 (d, $J = 8.0$ Hz, 1H), 6.35 (s, 2H), 3.90 (s, 3H), 3.80 (s, 6H), 2.35 (s, 3H); LRMS: EI+ 392 (M+1, 30%).

4.1.7. Compound **6e**

Color: yellow solid (61%); $R_f = 0.64$ (50% ethyl acetate/hexane); mp 107–109 °C; IR (KBr disc)/cm⁻¹ 2936, 2827, 1866, 1841, 1789, 1737, 1721, 1710, 1680, 1666, 1660, 1651, 1644, 1632, 1613, 1581, 1557, 1537, 1531, 1503, 1486, 1462, 1416, 1351, 1272, 1238, 1125, 980; ¹H NMR (400 MHz, CDCl₃): δ 7.52 (s, 1H), 7.32 (d, $J = 8.0$ Hz, 2H), 6.95 (d, $J = 8.0$ Hz, 2H), 6.35 (s, 2H), 3.84 (s, 3H), 3.78 (s, 6H), 2.35 (s, 3H); LRMS: EI+ 390 (100% M⁺).

4.1.8. Compound **6f**

Color: colorless oil (91%); $R_f = 0.22$ (50% ethyl acetate/hexane); IR (KBr disc)/cm⁻¹ 3404, 3087, 3062, 3000, 2939, 2837, 1959, 1939, 1710, 1672, 1588, 1537, 1505, 1462, 1455, 1414, 1355, 1325, 1276, 1237, 1198, 1183, 1126, 1041, 1005, 976, 956, 913, 881, 830, 754, 680, 666; ¹H NMR (400 MHz, CDCl₃): δ 7.54 (s, 1H), 7.46 (d, $J = 8.0$ Hz, 2H), 7.18 (d, $J = 8.0$ Hz, 2H), 6.34 (s, 2H), 3.92 (s, 3H), 3.78 (s, 6H), 2.36 (s, 3H); LRMS: EI+ 337 (100% M⁺).

4.1.9. Compound **6g**

Color: light yellow solid (31%); $R_f = 0.5$ (50% ethyl acetate/hexane); mp 88–90 °C; IR (KBr disc)/cm⁻¹ 2997, 2940, 2836, 1709, 1682, 1504, 1462, 1422, 1354, 1334, 1312, 1281, 1238.82, 1181, 1156, 1126, 1042, 1007; ¹H-NMR (400 MHz, CDCl₃): δ 7.57 (s, 1H), 7.08 (dd, $J = 4.0$ Hz, 8.0 Hz, 2H), 6.90 (t, $J = 8.0$ Hz, 2H), 6.37 (s, 2H), 3.92 (s, 3H), 3.79 (s, 6H), 2.36 (s, 3H); LRMS: EI+ 330 (100% M⁺).

4.1.10. Compound **6h**

Color: yellow oil (55%); $R_f = 0.6$ (50% ethyl acetate/hexane); IR (KBr disc)/cm⁻¹ 3070, 3001, 2936, 2836, 1681, 1661, 1598, 1580, 1509, 1461, 1410, 1353, 1298, 1237, 1174, 1125, 1026, 975, 952, 921, 880, 830, 758, 698, 681, 666; ¹H NMR (400 MHz, CDCl₃): δ 7.59 (s, 1H), 7.04 (d, $J = 8.0$ Hz, 2H), 6.73 (d, $J = 8.0$ Hz, 2H), 6.39 (s, 2H), 3.92 (s, 3H), 3.79 (s, 6H), 3.78 (s, 3H), 2.35 (s, 3H); LRMS: EI+ 342 (100% M⁺); HRMS: obs = 342.1471; calcd = 342.1467.

4.1.11. Compound **6i**

Color: yellow oil (27%); $R_f = 0.26$ (50% ethyl acetate/hexane); IR (KBr disc)/cm⁻¹ 2999, 2938, 2837, 1681, 1667, 1595, 1581, 1538,

1504, 1485, 1463, 1438, 1411, 1353, 1315, 1297, 1238, 1196, 1179, 1163, 1125, 1048, 1024, 1007, 880, 824, 776, 755, 696; $^1\text{H NMR}$ (400 MHz, CDCl_3): δ 7.98 (s, 1H), 7.20 (t, $J = 8.0$ Hz, 1H), 6.86 (d, $J = 8.0$ Hz, 1H), 6.76 (d, $J = 8.0$ Hz, 1H), 6.62 (t, $J = 8.0$ Hz, 1H), 3.88 (s, 3H), 3.87 (s, 3H), 3.72 (s, 6H), 2.43 (s, 3H); LRMS: EI+ 342 (100% M^+).

4.1.12. Compound 6j

Color: yellow oil (41%); $R_f = 0.28$ (50% ethyl acetate/hexane); IR (KBr disc)/ cm^{-1} 3051, 2998, 2936, 2833, 1666, 1596, 1581, 1558, 1537, 1531, 1503, 1488, 1462, 1432, 1410, 1352, 1313, 1260, 1237, 1158, 1125, 1042, 1006, 911, 876, 783, 751, 694, 666; $^1\text{H NMR}$ (400 MHz, CDCl_3): δ 7.59 (s, 1H), 7.14 (t, $J = 8.0$ Hz, 1H), 6.60–6.80 (m, 1H), 6.59 (s, 1H), 6.40 (s, 2H), 3.90 (s, 3H), 3.79 (s, 6H), 3.54 (s, 3H), 2.38 (s, 3H); LRMS: EI+ 342 (100% M^+).

4.1.13. Compound 6k

Color: yellow solid (48%); $R_f = 0.6$ (50% ethyl acetate/hexane); mp 102–104 °C; IR (KBr disc)/ cm^{-1} 2997, 2928, 2835, 1667, 1581, 1505, 1456, 1411, 1348, 1317, 1236, 1183, 1123, 1008, 813; $^1\text{H NMR}$ (400 MHz, CDCl_3): δ 7.60 (s, 1H), 7.02 (d, $J = 8.0$ Hz, 2H), 6.99 (d, $J = 8.0$ Hz, 2H), 6.38 (s, 3H), 3.92 (s, 3H); 3.78 (s, 6H); 2.37 (s, 3H); 2.30 (s, 3H); LRMS: EI+ 326 (100% M^+); HRMS: obs = 326.1515; calcd = 326.1518.

4.1.14. Compound 6l

Color: light yellow oil (29%); $R_f = 0.3$ (50% ethyl acetate/hexane); IR (KBr disc)/ cm^{-1} 3059, 3022, 2998, 2937, 2831, 2592, 2469, 2426, 2360, 2247, 2147, 1964, 1841, 1789, 1737, 1681, 1666, 1580, 1537, 1503, 1462, 1448, 1410, 1386, 1354, 1327, 1303, 1286, 1235, 1197, 1182, 1125, 1077, 1020, 1005, 953, 773, 757, 679; $^1\text{H NMR}$ (400 MHz, CDCl_3): δ 7.60 (s, 1H), 7.25–7.16 (m, 3H), 7.09 (d, $J = 4.0$ Hz, 2H), 6.38 (s, 2H), 3.90 (s, 3H), 3.75 (s, 6H), 2.37 (s, 3H); LRMS: EI+ 312 (100% M^+).

4.1.15. Compound 6m

Color: yellow oil (90%); $R_f = 0.44$ (50% ethyl acetate/hexane); IR (KBr disc)/ cm^{-1} 2359, 1658, 1652, 1581, 1557, 1538, 1504, 1462, 1455, 1410, 1378, 1353, 1316, 1277, 1236, 1126, 1026, 1003, 916, 883, 819, 698, 695; $^1\text{H NMR}$ (400 MHz, CDCl_3): δ 7.47 (s, 1H), 7.24 (d, $J = 8.0$ Hz, 2H), 7.19 (d, $J = 4$ Hz, 1H), 6.87–9.0 (dd, 1H), 6.38 (s, 2H), 3.91 (s, 3 H), 3.79 (s, 6H), 2.35 (s, 3H); LRMS: EI+ 380 (100% M^+).

4.1.16. Compound 6n

Color: orange solid (85%); $R_f = 0.25$ (50% ethyl acetate/hexane); mp 88–90 °C; IR (KBr disc)/ cm^{-1} 2998, 2940, 2840, 1709, 1666, 1613, 1581, 1530, 1504.0, 1461, 1412, 1353, 1281.49, 1236, 1198, 1184, 1159, 1123, 1088, 1010, 820, 755, 733, 619; $^1\text{H NMR}$ (400 MHz, CDCl_3): δ 7.62 (s, 1H), 7.51 (s, 1H), 7.22–7.20 (dd, 1H), 6.90 (d, $J = 8.0$ Hz, 1H), 6.38 (s, 2H), 3.94 (s, 3H), 3.93 (s, 3H), 3.81 (s, 3H), 2.35 (s, 3H); LRMS: EI+ 387 (100% M^+); HRMS: obs = 387.1311, calcd = 387.1318.

4.1.17. Compound 6o

Color: yellow oil (81%); $R_f = 0.33$ (50% ethyl acetate/hexane); IR (KBr disc)/ cm^{-1} 3000, 2938, 2831, 1684, 1666, 1598, 1582, 1506, 1462, 1454, 1413, 1385, 1354, 1318, 1302, 1287, 1235, 1195; $^1\text{H NMR}$ (400 MHz, CDCl_3): δ 8.01 (s, 1H), 6.80 (d, $J = 4.0$ Hz, 2H), 6.40 (s, 2H), 6.36 (d, $J = 4.0$ Hz, 1H), 3.86 (s, 6H), 3.77 (s, 6H), 3.34 (s, 3H), 2.45 (s, 3H); LRMS: EI+ 372 (75%, M^+).

4.1.18. Compound 6p

Color: yellow oil (91%); $R_f = 0.66$ (50% ethyl acetate/hexane); IR (KBr disc)/ cm^{-1} 3001, 2935, 2835, 1712, 1659, 1581, 1512, 1462, 1415, 1353, 1334, 1306, 1268, 1239, 1162, 1125, 1023, 879, 858,

809, 752, 667, 680; $^1\text{H NMR}$ (400 MHz, CDCl_3): δ 7.59 (s, 1H), 6.91–6.88 (dd, 1H), 6.76 (d, $J = 8.0$ Hz, 1H), 6.52 (s, 1H), 6.45 (s, 2H), 3.88 (s, 3H), 3.85 (s, 3H), 3.81 (s, 6H), 3.49 (s, 3H), 2.37 (s, 3H); LRMS: EI+ 372 (100% M^+).

4.1.19. Compound 6q

Color: yellow oil (72%); $R_f = 0.61$ (50% ethyl acetate/hexane); IR (KBr disc)/ cm^{-1} 2998, 2938, 2838, 1955, 1709, 1667, 1601, 1504, 1461, 1414, 1351, 1335, 1298, 1234, 1207, 1183, 1156, 1127, 1058, 1033, 1006, 951, 815, 751, 733, 685; $^1\text{H NMR}$ (400 MHz, CDCl_3): δ 7.59 (s, 1H), 6.28 (s, 2H), 5.98 (s, 2H), 3.80 (s, 3 H), 3.77 (s, 3H), 3.65 (s, 6H), 3.51 (s, 6H), 2.50 (s, 3H); LRMS: EI+ 402 (100% M^+).

4.1.20. Compound 6r

Color: yellow oil (96%); $R_f = 0.4$ (50% ethyl acetate/hexane); IR (KBr disc)/ cm^{-1} 2997, 2937, 2835, 1707, 1681, 1663, 1578, 1502, 1459, 1419, 1330, 1237, 1184, 1157, 1125, 1039, 1003, 953, 924, 880, 833, 753, 695, 670; $^1\text{H NMR}$ (400 MHz, CDCl_3): δ 7.54 (s, 1H), 6.45 (s, 2H), 6.40 (s, 2H), 3.87 (s, 3H), 3.83 (s, 3H), 3.82 (s, 6H), 3.61 (s, 6H), 2.37 (s, 3H); LRMS: EI+ 402 (M^+ , 100%).

4.1.21. Compound 6s

Color: brown oil (42%); $R_f = 0.5$ (50% ethyl acetate/hexane); IR (KBr disc)/ cm^{-1} 2996, 2938, 2848, 1710, 1662, 1584, 1507, 1456, 1418, 1238, 1127, 1005, 844, 782, 762, 717; $^1\text{H NMR}$ (400 MHz, CDCl_3): δ 7.53 (s, 1H), 6.83 (d, $J = 8$ Hz, 1H), 6.72 (d, $J = 8$ Hz, 1H), 6.56 (s, 1H), 3.90 (s, 3H), 3.78 (s, 6H), 3.77 (s, 3H) 2.30 (s, 3H), 0.89 (s, 9H), 0.07 (s, 6H); LRMS: EI+ 472 (M^+ , 30%).

4.1.22. Compound 6t

Color: light yellow solid (48%); $R_f = 0.25$; (50% ethyl acetate/hexane); mp 113–115 °C; IR (KBr disc)/ cm^{-1} 3014, 2937, 2843, 1661, 1583, 1508, 1457, 1411, 1350, 1277, 1237, 1126, 1018, 758, 668; $^1\text{H NMR}$ (400 MHz, CDCl_3): δ 7.51 (s, 1H), 6.62–6.67 (m, 3H), 6.37 (s, 2H), 5.46 (s, 1H), 3.91 (s, 3H), 3.86 (s, 3H), 3.79 (s, 6H), 2.32 (s, 3H); LRMS: EI+ 358 (M^+ , 100%); HRMS: obs = 358.1423; calcd = 358.1416.

4.2. Biological studies

4.2.1. Cytotoxicity studies on L1210 murine lymphoma and B16-F0 melanoma cell lines

The L1210 and B16-F0 cell lines were obtained from American Type Tissue Culture Collection (ATCC) and the MMT based cytotoxicity studies were conducted exactly according to a recently published procedure.^{7,17}

4.2.2. NCI in vitro cytotoxicity screen

Compound **6t** was also tested against a panel of 60 human cancer cell lines at the National Cancer Institute, Bethesda, MD.^{13a} The cytotoxicity studies were conducted using a 48 h exposure protocol using the sulforhodamine B assay.^{13b} Dose–response curves were used to generate the GI_{50} (concentration of drug needed to inhibit the growth by 50%), TGI (total growth inhibition), and LC_{50} values (concentration needed to inhibit the growth of cells by 50%).

4.2.3. Toxicity studies of compounds 6k and 6t on healthy female DBA2 mice

Compound **6k** and **6t** was formulated by mixing the appropriate amount of the compound with 1.5 mL of PET (polyethylene glycol 400, absolute ethanol, and Tween 80 in 6:3:1 portions), 1.2 mL of 5% glucose in water, and 0.3 mL of DMSO for **6t** and 0.6 mL of DMSO for **6k**. The final concentration of ethanol was 15% and DMSO 10%. In each case clear, colorless solutions were obtained. Using an average weight of a mouse of 20 g, a 100 μL (for **6t**) and

110 μL (for **6k**) injection of this solution provided a dose of 75 mg/kg. The solution was stored at 20 °C and the compound's stability was monitored by TLC analysis.

Week (5–7) old female DBA2 mice obtained from the Jackson Laboratory were treated via an intraperitoneal (IP) route using the abovementioned formulation. Five mice were included in each group. Injections were made on days 1, 5, 9, 13 and 17. The control animals received only the vehicle (100 μL). Body weights were measured every other day and at the end of the experiment (day 23) the animals were sacrificed. The blood was analyzed by Kentwood Veterinary Hospital, Grand Rapids, MI and the appearance and weights of the internal organs (liver, kidney, spleen) were also examined.¹⁸

4.2.4. In vivo antitumor activity of 6k and 6t against L1210 murine lymphocytic leukemia¹⁸

Week (5–7) old female DBA2 mice were used in this study. Groups of four mice were inoculated with L1210 cells that have been passaged through a mouse. The cells were washed three times with PBS and resuspended in PBS at a concentration of 4.0×10^6 cells/mL. The cell suspensions (100 μL) were delivered subcutaneously (sc) to the left flank at day 0. At this concentration, each mouse received 200,000 tumor cells. The length and width of the tumors were measured almost every other day using a digital calipers and the tumor volume was calculated as: tumor volume (mm^3) = [length (mm) \times (width (mm))²]/2.

The drug solution was formulated as described. Each mouse received 100 μL (for **6t**) and 110 μL (for **6k**) of the drug solution via an intraperitoneal (ip) administration route on days 1, 3, 5, 7, 9, 11, 13, 15 and 17. Each injection delivered 50 mg/kg of compound **6k** and **6t**. Animal weights were taken every other day. The vehicle control group of mice was treated on a similar schedule with 100 μL of the vehicle.

Acknowledgments

The authors thank Conjura Pharmaceuticals, LLC for supporting this project (M.L.). Support from the President's Council Excellence award is acknowledged (S.L.M.).

Supplementary data

Supplementary data associated with this article can be found, in the online version, at doi:10.1016/j.bmc.2011.02.018.

References and notes

- (a) Pettit, G. R.; Singh, S. B.; Niven, M. L.; Hamel, E.; Schmidt, J. M. *J. Nat. Prod.* **1987**, *50*, 119; (b) Dorr, R. T.; Dvorakova, K.; Snead, K.; Alberts, D. S.; Salmon, S. E.; Pettit, G. R. *Invest. New Drugs* **1996**, *14*, 131.
- (a) Hsieh, H. P.; Liou, J. P.; Lin, Y. T.; Mahindroo, N.; Chang, J. Y.; Yang, Y. N.; Chern, S. S.; Tan, U. K.; Chang, C. W.; Chen, T. W.; Lin, C. H.; Chang, Y. Y.; Wang, C. C. *Bioorg. Med. Chem. Lett.* **2003**, *13*, 101; (b) Pettit, G. R.; Singh, S. B.; Boyd, M. R.; Hamel, E.; Pettit, R. K.; Schmidt, J. M.; Hogan, F. J. *Med. Chem.* **1995**, *38*, 1666.
- McGown, A. T.; Fox, B. W. *Cancer Chemother. Pharmacol.* **1990**, *26*, 79.
- (a) Tozer, G. M.; Prise, V. E.; Wilson, J.; Locke, R. J.; Vojnovic, B.; Stratford, M. R. L.; Dennis, M. F.; Chaplin, D. J. *Cancer Res.* **1999**, *59*, 1626; (b) Pero, R. W.; Sherris, D. *Chem. Abstr.* **2000**, *133*, 198575; (c) Tozer, G. M.; Kanthrou, C.; Parkins, C. S.; Hill, S. A. *Int. J. Exp. Pathol.* **2002**, *83*, 21; (d) Siemann, D. W.; Mercer, E.; Lepler, S.; Rojiani, A. M. *Int. J. Cancer* **2002**, *99*, 1.
- Galbraith, S. M.; Maxwell, R. J.; Lodge, M. A.; Tozer, G. M.; Wilson, J.; Taylor, N. J.; Stirling, J. J.; Sena, L.; Padhani, A. R.; Rustin, G. S. *J. Clin. Oncol.* **2003**, *15*, 2831.
- Wu-Wong, J. R.; Alder, J. D.; Alder, J. D.; Burns, D. J.; Han, E. K.-H.; Credro, B.; Tahir, S. K.; Dayton, B. D.; Ewing, P. J.; Chiou, W. J. *Cancer Res.* **2001**, *61*, 1486.
- (a) LeBlanc, R.; Dickson, J.; Brown, T.; Stewart, M.; Pati, H. N.; Van Derveer, D.; Arman, H.; Harris, J.; Pennington, W.; Holt, H.; Lee, M. *Bioorg. Med. Chem.* **2005**, *13*, 6025; (b) Johnson, M.; Younglove, B.; Lee, L.; LeBlanc, R.; Holt, H.; Patrice, H.; Mackay, H.; Brown, T.; Mooberry, S. L.; Lee, M. *Bioorg. Med. Chem. Lett.* **2007**, *17*, 5897; (c) Lee, L.; Davis, R.; Vanderham, J.; Hills, P.; Mackay, H.; Brown, T.; Mooberry, S. L.; Lee, M. *Eur. J. Med. Chem.* **2008**, *43*, 2011; (d) Chavda, S.; Davis, R.; Ferguson, A.; Riddering, C.; Dittenhafer, K.; Mackay, H.; Babu, B.; Lee, M.; Siegfried, A.; Pennington, W.; Shadfan, M.; Mooberry, S. L.; Mishra, B. K.; Pati, H. N. *Letts. Drug Des. Disc.* **2009**, *7*, 531; (e) Lee, L.; Lyda, M. R.; Lee, M.; Davis, R.; Mackay, H.; Chavda, S.; Babu, B.; O'Brien, E. L.; Risinger, A. L.; Mooberry, S. L.; Lee, M. *J. Med. Chem.* **2010**, *53*, 325.
- Gaukoger, K.; Hadfield, J. A.; Hepworth, L. A.; Lawrence, N. J.; McGown, A. T. *J. Org. Chem.* **2001**, *66*, 8135.
- Takeya, T.; Okubo, T.; Nishida, S.; Tobinaga, S. *Chem. Pharm. Bull.* **1985**, *33*, 3599.
- Ruprich, J.; Prout, A.; Dickson, J.; Younglove, B.; Nolan, L.; Baxi, K.; LeBlanc, R.; Forrest, L.; Hills, P.; Holt, H.; Mackay, H.; Brown, T.; Mooberry, S.; Lee, M. *Letts. Drug Des. Disc.* **2007**, *4*, 144.
- (a) Lara-Ochoa, F.; Espinosa-Perez, G. *Tetrahedron Lett.* **2007**, *48*, 7007; (b) Pettit, G. R.; Rhodes, M. R.; Herald, D. L.; Hamel, E.; Schmidt, J. M.; Pettit, R. K. *J. Med. Chem.* **2005**, *4*, 4087.
- Kupchinsky, S.; Centioni, S.; Howard, T.; Trzupke, J.; Roller, S.; Carnahan, V.; Townes, H.; Purnell, B.; Price, C.; Handl, H.; Summerville, K.; Johnson, K.; Toth, J.; Hudson, S.; Kiakos, K.; Hartley, J. A.; Lee, M. *Bioorg. Med. Chem.* **2004**, *12*, 6221.
- (a) Boyd, R. B. The NCI In Vitro Anticancer Drug Discovery Screen. In *Anticancer Drug Development Guide: Preclinical Screening, Clinical Trials, and Approval*; Teicher, B., Ed.; Humana Press Inc.: Totowa, NJ, 1997; pp 23–42; (b) Kehan, P.; Storeng, R.; Scudiero, D.; Monks, A.; McMahon, J.; Vistica, D., et al. *J. Natl. Cancer Inst.* **1990**, *82*, 1107.
- Blagosklonny, M. V.; Darzynkiewicz, Z.; Halicka, H. D.; Pozarowski, P.; Demidenko, Z. N.; Barry, J. J.; Kamath, K. R.; Herrmann, R. A. *Cell Cycle* **2004**, *3*, 1048.
- (a) Cox, C.; Breslin, M.; Mariano, B.; Coleman, P.; Buser, C.; Walsh, E.; Hamilton, K.; Huber, H.; Kohl, N.; Torrent, M.; Yan, Y.; Kuo, L.; Hartman, G. *Bioorg. Med. Chem. Lett.* **2005**, *15*, 2041; (b) Fraley, M.; Garbaccio, R. M.; Arrington, K. L.; Hoffman, W. F.; Tasber, E. S.; Coleman, P. J.; Buser, C. A.; Walsh, E. S.; Hamilton, K.; Fernandes, C.; Schaber, M. D.; Lobell, R. B.; Tao, W.; South, V. J.; Yan, Y.; Kuo, L.; Prueksaritanont, T.; Shu, C.; Torrent, M.; Heimbrook, D. C.; Kohl, N. E.; Huber, H. E.; Hartman, G. D. *Bioorg. Med. Chem. Lett.* **2006**, *16*, 1775; (c) Garbaccio, R. M.; Fraley, M. E.; Tasber, E. S.; Olson, C. M.; Hoffman, W. F.; Arrington, K. L.; Torrent, M.; Buser, C. A.; Walsh, E. S.; Hamilton, K.; Schaber, M. D.; Fernandes, C.; Lobell, R. B.; Tao, W.; South, V. J.; Yan, Y.; Kuo, L. C.; Prueksaritanont, T.; Slaughter, D. E.; Shu, C.; Heimbrook, D. C.; Kohl, N. E.; Huber, H. E.; Hartman, G. D. *Bioorg. Med. Chem. Lett.* **2006**, *16*, 1780.
- Gupton, J. T.; Burham, B. S.; Krumpke, K.; Du, K.; Sikorski, J. A.; Warren, A. E.; Barnes, C. R.; Hall, I. H. *Arch. Pharm. (Weinheim)* **2000**, *333*, 3.
- Carmichael, J.; Degraff, W. G.; Gazdar, A. F.; Minna, J. D.; Mitchell, J. B. *Cancer Res.* **1987**, *47*, 936.
- Sato, A.; McNulty, L.; Cox, K.; Kim, S.; Scott, A.; Daniell, K.; Summerville, K.; Price, C.; Hudson, S.; Kiakos, K.; Hartley, J. A.; Asao, T.; Lee, M. *J. Med. Chem.* **2005**, *48*, 3903.